ADJOINT-BASED SHAPE OPTIMIZATION FOR A SEMI-SUBMERGED ENGINE INLET

Umut Can Küçük[*]
Turkish Aerospace
Ankara, Turkey

İsmail Hakkı Tuncer[†]
Middle East Technical University
Ankara, Turkey

ABSTRACT

In this study, adjoint-based optimization is conducted for increasing the performance of a semi-submerged inlet exposing a large amount of boundary layer ingestion. Flow and adjoint solutions are conducted with the open-source software SU^2. In the optimizations, the highlight area and its shape, overall diffusion ratio and vertical offset are kept constant and total pressure recovery is maximized. Results indicate that the surface modifications obtained with the optimization algorithm lead to a performance increase both in design and off-design conditions. It is further shown that this performance increase is mostly generated by diverting the upcoming boundary layer away from the inlet entrance.

INTRODUCTION

The main purpose of an engine inlet is to capture a sufficient amount of external flow and transport it to the engine with the highest uniformity and lowest loss. The location and orientation of an engine inlet on an air vehicle body play a crucial role in both aerodynamic performance and survivability of the overall system. In military applications, it is common to compromise the aerodynamic performance of an air inlet in exchange for achieving lower radar cross-section and higher compactness. On the other hand, in the commercial aircraft business, engine inlets are generally placed and oriented so that the aerodynamic performance of an intake is maximized. Recently, boundary layer ingesting (BLI) propulsion systems take the attention of commercial aircraft businesses thanks to their possible benefits in increasing overall propulsion system efficiency and reducing external drag by embedding inlets into the airframe. However, placing the engine inlet in a coupled manner with the aircraft body and/or shielding engine components from radar waves can lead to a significant reduction in air inlet aerodynamic performance. These types of engine inlets are now designed without diverters and splitter plates so that part of the boundary layer flow developed on the fuselage is ingested. The ingestion of the boundary layer increases negative effects associated with high adverse pressure gradients in radial and axial directions of the compact engine inlets with centerline curvature. Therefore, the design of a boundary layer ingesting inlet is a challenging task.

In this study, adjoint-based optimization is conducted for a boundary layer ingesting inlet in transonic

---

[*]An Aerospace Engineer, Email: kucukumutcan@gmail.com

[†]Professor in Aerospace Engineering Department, Email: ismail.h.tuncer@ae.metu.edu.tr

flow conditions. The investigated inlet is taken from the experimental study. Flow and adjoint computations are carried out with the open-source software SU^2. For the geometrical parametrization, the free-form deformation (FFD) approach is used with a large number of design variables. The obtained geometry from the optimization shows a significant performance increase both in design and off-design conditions.

METHOD

In this study adjoint-based optimization is carried out for increasing the performance of a boundary layer ingesting inlet. The inlet geometry is obtained from a comprehensive experimental study [Bobby et al., 2005]. The same geometry is previously investigated by the authors [Kucuk and Tuncer, 2022]. In the earlier study, verification of the computational approach and adjoint-based optimization is conducted so that, inlet geometry starting from the inlet throat is optimized with 225 design variables. Results of the previous investigation show that the losses inside the engine inlet are small and optimizing the engine inlet only leads to a small amount of performance increase. In this study, optimization is conducted so that the throat area is also allowed to change and the number of design variables is increased. Now, the geometrical deformations are allowed to start just after the leading edge of the inlet lips so that the highlight area is kept constant rather than the inlet throat and total pressure recovery of the engine inlet is maximized with adjoint-based optimization. The computational approaches followed for the flow and adjoint-based gradient evaluations are briefly described in this paper. The reader is referred to the recently published Ph.D. Thesis [Kucuk, 2022] for detailed explanations.

For the flow and adjoint-based solutions, open-source SU^2 software is used. The gradient-based optimization is driven by the Sequential least square programming which is also embedded in the SU^2 software.

Flow and Adjoint Solver: SU^2

SU^2 is an open-source software developed for solving partial differential equations on unstructured grids. The core of the software is the Reynolds Averaged Navier Stokes solver which can be used for simulating a wide range of flow regimes. One of the key features of the SU^2 software is related to its capability to perform adjoint optimizations for aerodynamic shapes. Within the SU^2 software, it is possible to obtain gradient information that can be used for an optimal shape design and it is also possible to perform mesh deformations and refinements.

In SU^2 solutions turbulence is modeled with the SA turbulence model. The Central Jameson-Schmidt-Turkel (JST) flux splitting method is utilized. Gradient calculations are based on the Green Gauss Theorem and the Venkatakrishnan slope limiter is used. Steady-state solutions are obtained with a CFL number of 15. In adjoint solutions, the Venkatakrishnan slope limiter is similarly used. The CFL reduction factor is set to 0.1.

Adjoint Formulation

The adjoint-based optimization algorithms provide the ability to efficiently deal with a large number of design variables. This is originating from the characteristic of adjoint optimization algorithms so that equations of the flow field become constraints so the final expression for the gradient does not require reevaluation of the flow field as shown by [Nadarajah and Jamesson, 2000]. A conceptual explanation of adjoint-based optimization is given below.

The cost function I, is depending on the vector of design variables, Γ, the flow field variable vector U, and grid position vector, X that is

$$I = I(U, X, \Gamma)$$

Similarly, the discrete residual vector, R, can be expressed as

$$R = R(U, X, \Gamma) = 0$$

2

since with the converged RANS solutions, the governing equations of flow must be satisfied. A chain rule can be applied to express the sensitivity derivatives of the objective function on the design variables

$$\frac{dI}{d\Gamma} = \frac{\partial I}{\partial U}\frac{dU}{d\Gamma} + \frac{\partial I}{\partial X}\frac{dX}{d\Gamma} + \frac{\partial I}{\partial \Gamma} \tag{1}$$

The term $\frac{dU}{d\Gamma}$ seen in the above equation can increase the cost of the optimization problem drastically if a large number of design variables are included. Therefore, adjoint variables are introduced so that this term can be eliminated. Accordingly, the discrete Residual is differentiated to obtain the Jacobian matrix.

$$\frac{dR}{d\Gamma} = \frac{\partial R}{\partial U}\frac{dU}{d\Gamma} + \frac{\partial R}{\partial X}\frac{dX}{d\Gamma} + \frac{\partial R}{\partial \Gamma} = 0 \tag{2}$$

Now, with the adjoint vector, λ, and grouping the $\frac{dU}{d\Gamma}$ term, equations 1 and 2 can be combined to obtain the below expression.

$$\frac{dI}{d\Gamma} = \frac{\partial I}{\partial X}\frac{dX}{d\Gamma} + \frac{\partial I}{\partial \Gamma} + \lambda^T\left(\frac{\partial R}{\partial X}\frac{dX}{d\Gamma} + \frac{\partial R}{\partial \Gamma}\right) + \left(\frac{\partial I}{\partial U} + \lambda^T\frac{\partial R}{\partial U}\right)\frac{dU}{d\Gamma} \tag{3}$$

Adjoint vector λ is selected so that

$$\left(\frac{\partial I}{\partial U} + \lambda^T\frac{\partial R}{\partial U}\right) = 0$$

is satisfied. Accordingly, the sensitivity equation (Equation 3) is greatly simplified to the following

$$\frac{dI}{d\Gamma} = \frac{\partial I}{\partial X}\frac{dX}{d\Gamma} + \frac{\partial I}{\partial \Gamma} + \lambda^T\left(\frac{\partial R}{\partial X}\frac{dX}{d\Gamma} + \frac{\partial R}{\partial \Gamma}\right)$$

so that sensitivity derivatives can be obtained without dependency on the flow variables. The sensitivities of the grid nodes with respect to the design variables, $dX/d\Gamma$, is then evaluated by means of the SU2_DOT_AD module, which is based on the differentiation of the mesh deformation code with FFD. The adjoint sensitivities with respect to the mesh coordinates, $\partial I/\partial X$ are all computed in one adjoint solution.

Inlet Performance Parameters and Optimization Goal

In this study, average circumferential distortion, $DPCP_{avg}$, total pressure recovery of the inlet, PR, and corrected mass flow rate at the aerodynamic interface plane, $\dot{m}_c$, are monitored. For the calculations of $DPCP_{avg}$ from the CFD solutions, a virtual total pressure rake, composed of 8 arms and 5 rings, is placed on the aerodynamic interface plane (AIP) based on the SAE standard by [Society of Automotive Engineers, 1978] and total pressure values at each of the probe locations are obtained. These total pressure readings are also used for the calculation of the Pressure Recovery which is the average total pressure at the AIP divided by the free stream total pressure. Although it is often the case that, maximizing total pressure on the engine face leads to a reduction in distortion, the designer must take into account and monitor these two parameters as explained by [Seddon and Goldsmith, 1985].

$DPCP_{avg}$ is simply the average of ring intensities given in Equation 4.

$$Intensity_i = \frac{P_{avg,i} - P_{l,avg,i}}{P_{avg,i}} \tag{4}$$

In the Equation 4 i, $P_{avg,i}$, $P_{l,avg,i}$ represents ring number, the average total pressure on the ring number i, average total pressure obtained in the low-pressure region on the ring number i respectively. Accordingly, $DPCP_{avg}$ is calculated by simply taking the average of intensities at each ring with the help of Equation 5.

$$DPCP_{avg} = \sum_{i=1}^{i=5} \frac{Intensity_i}{5} \tag{5}$$

The corrected mass flow rate can be expressed with Equation 6 where $\dot{m}$ is the real mass flow rate going through the inlet, Tt and Pt_{AIP} are total temperature and total pressure at the AIP. For the correction, T_{ref} and P_{ref} are taken as 288.15 K and 101325 Pa respectively.

$$\dot{m}_c = \dot{m} \frac{\sqrt{\frac{Tt}{Tref}}}{\frac{Pt_{AIP}}{Pref}} \tag{6}$$

RESULTS AND DISCUSSION

In this study, the effect of 6699 design variables on the total pressure recovery of a semi-submerged inlet is calculated with the adjoint method. Parametrization of the geometry is performed with a Free Form Deformation box defined with bezier volume. During the optimization study, the total pressure recovery of the inlet is maximized while the corrected mass flow rate is monitored. In addition, circumferential distortion for the optimum inlet is compared with the baseline geometry. The performance of the optimum geometry is also investigated at off-design conditions characterized by different levels of mass flow rates.

Free Form Deformation (FFD) Box

The FFD box used in this study, shown in Figure 1, starts from the leading edge of the inlet and ends just upstream of the aerodynamic interface plane(AIP). It contains 31 planes in the axial direction, 21 planes in the lateral direction and 11 planes in the vertical direction. The first and the last axial planes of the FFD box are kept constant so that the highlight area, AIP and vertical offset of the inlet are not modified. Accordingly, the number of design variables included in the optimization study is 6699.
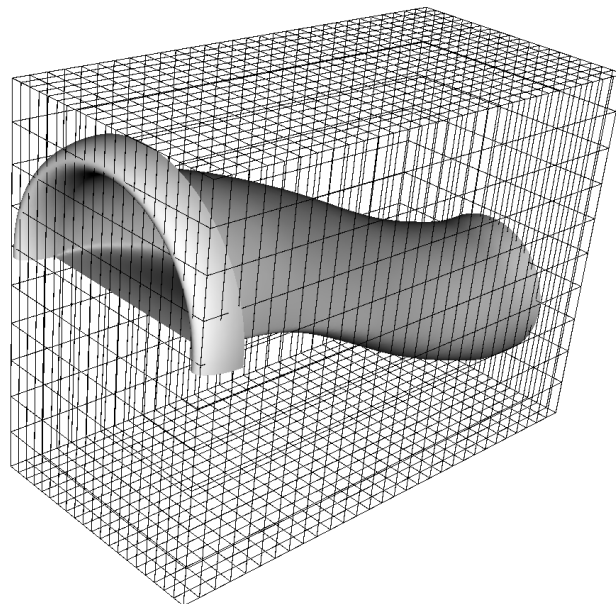
Figure 1: FFD Box

Optimization History

The variation of the Pressure Recovery and mass flow rate with respect to the optimization steps are

shown in Figure 2. As seen, in the early stages of the optimization significant increase in pressure recovery values is observed and this increase is accompanied by an increase in mass flow rate.

(a) Pressure Recovery Change

(b) Corrected Mass Flow Rate Change
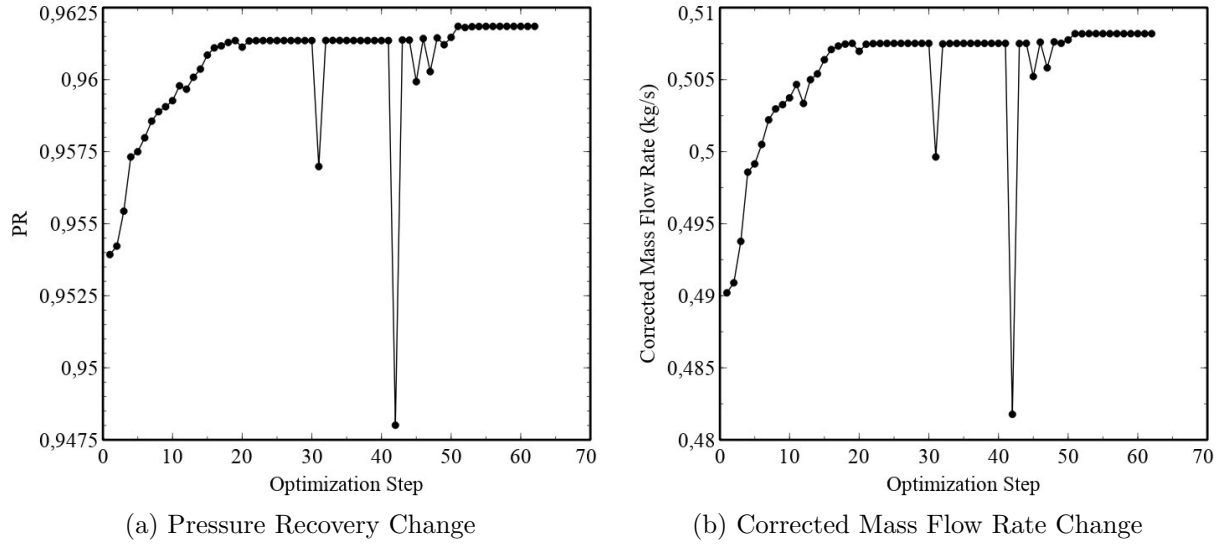
Figure 2: Optimization History

Optimum Performance and Geometry

The comparison of the baseline and optimum inlet geometries is given in Figure 3. As seen, observable change at the inlet entrance is obtained so that the bottom wall of the inlet at the corners is escalated by the optimization algorithm. After the inlet entrance, the cross-sectional areas are enlarged while the egg-shaped cross-sectional shapes are preserved. The effect of these geometrical variations on the static pressure distribution at the mid-plane of the duct is given in Figure 4 and the performance comparison of the optimum and baseline inlet are presented in Table 1. As seen, a significant performance increase at the design condition is obtained so that PR and mass flow rate are increased while a more than 13 % decrease in distortion is obtained.

Table 1: Performance parameters for Case 1

	Optimum	Baseline	% Difference
PR	0.962	0.954	0.82
$\dot{m}_c$ (kg/s)	0.508	0.492	3.32
$DPCP_{avg}$	0.046	0.053	-13.21

Pressure recovery contours obtained from optimum and baseline inlet are also compared in Figure 5 which shows that the spoiled sector at the AIP is shrunk by the optimization algorithm. Pressure recovery distributions at the symmetry plane and cross sections through the stream-wise direction are also compared in Figure 6 for the baseline and the optimum inlet. As seen escalating the bottom wall of the inlet at the entrance reduces the ingested amount of flow with low total pressure. This can also be seen in Figure 7 showing the surface streamlines are diverted away from the optimum inlet entrance. This effect is created with the increased static pressure by escalating the ground walls at the corners of the inlet entrance.
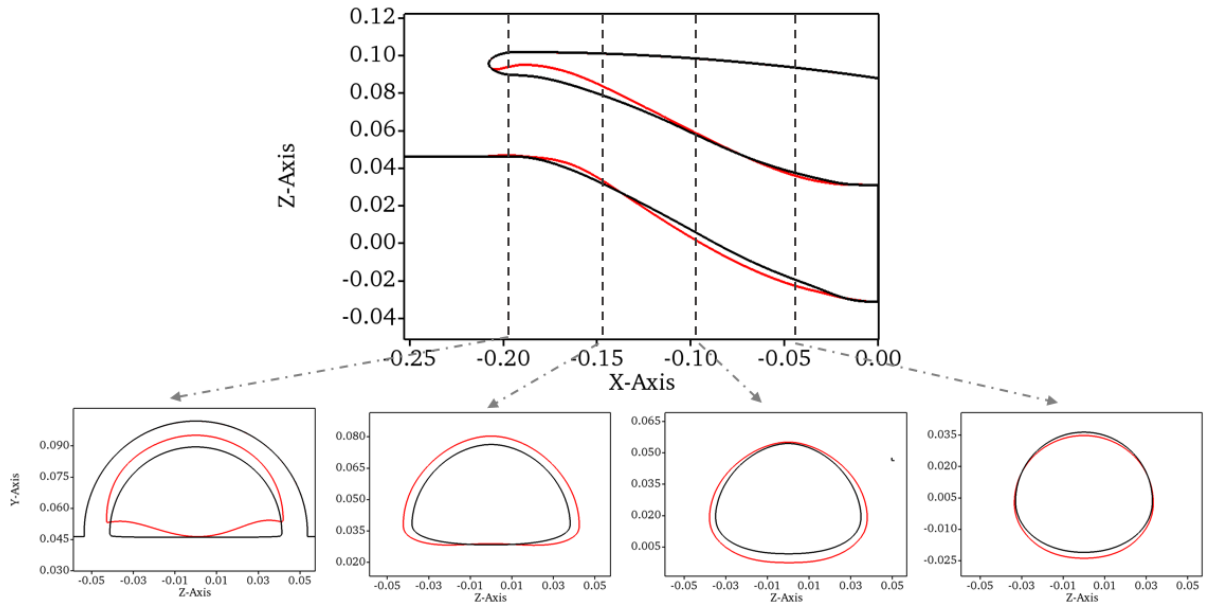
Figure 3: Geometrical Variations (Red is Optimum and Black is Baseline Geometry)
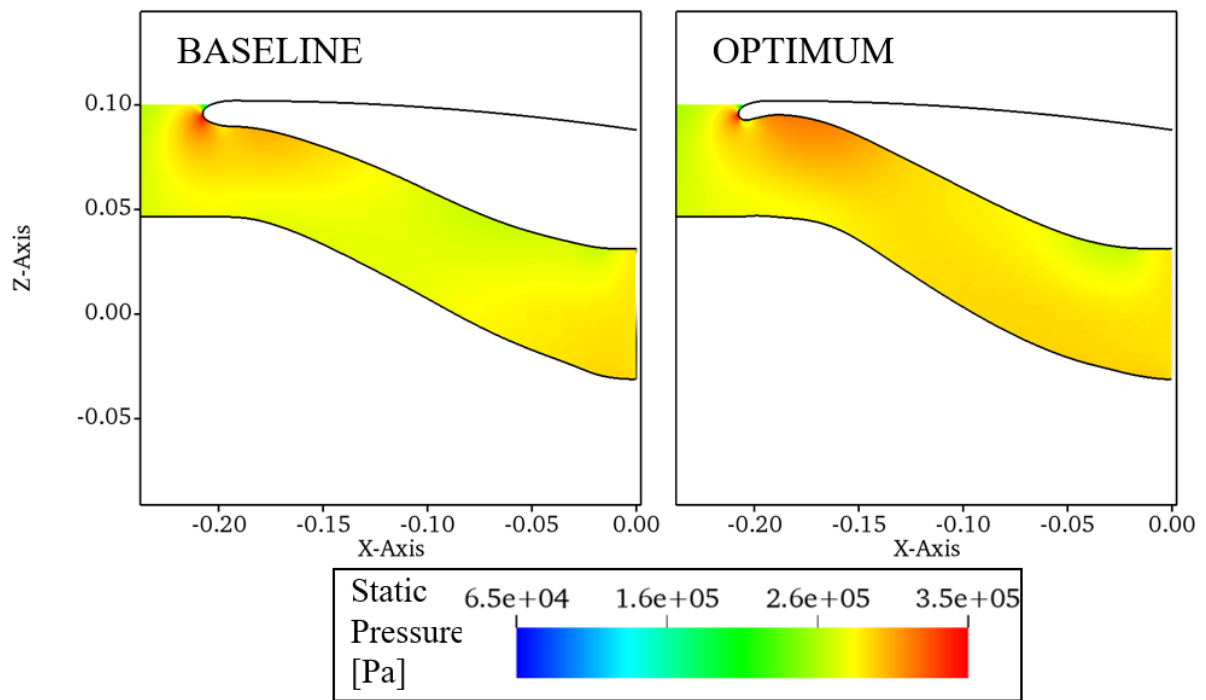
Figure 4: Static Pressure Distributions at the Symmetry Plane
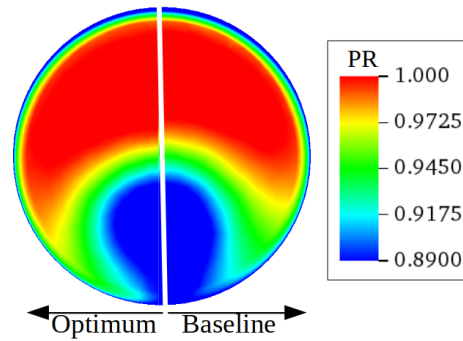
Figure 5: Pressure Recovery Distribution Comparison at the AIP
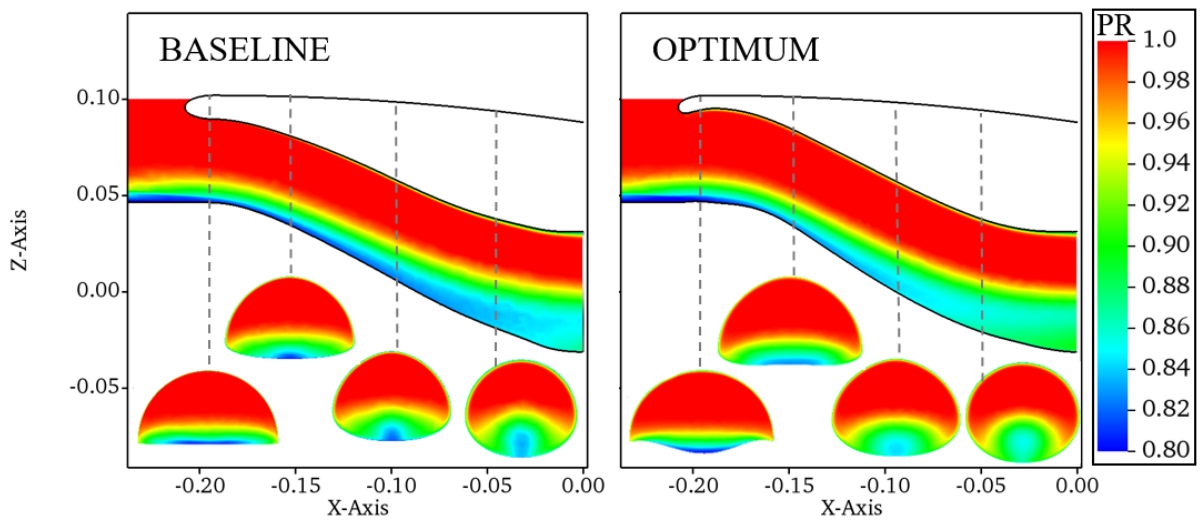
Figure 6: Total Pressure Recovery Distributions
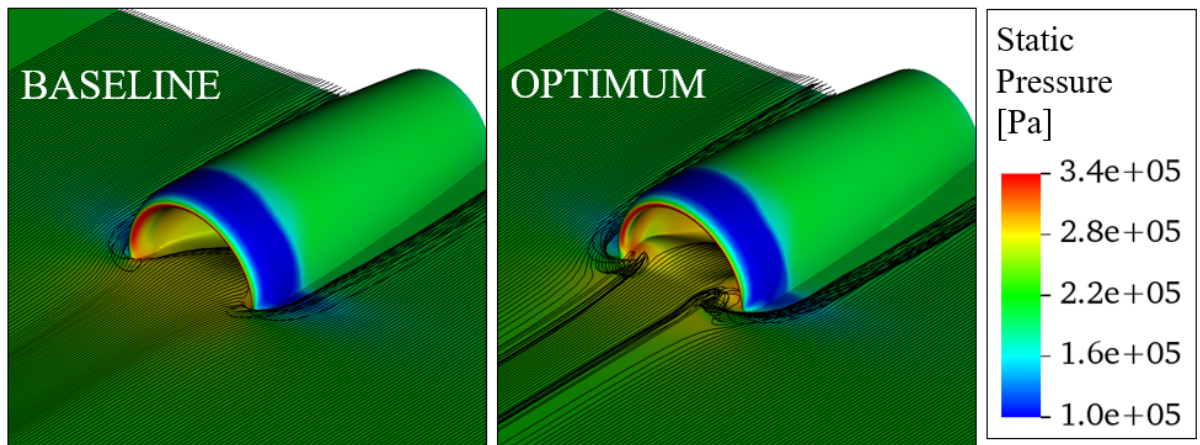
Figure 7: Surface Streamlines with Static Pressure on the Walls

Off-Design Performances

The optimization is conducted at a single flow condition. However, the behavior of the engine inlet under off-design conditions must also be investigated since the designed inlet will be exposed to different flow conditions. These flow conditions can be characterized by the different levels of mass flow rate. Accordingly, a set of flow analyses are conducted for both baseline and optimum configurations and their performances are compared in Figure 8. As seen, the optimum configuration provides a significant performance increase for a wide range of mass flow rates.

(a) Pressure Recovery Comparison   (b) Distortion Comparison
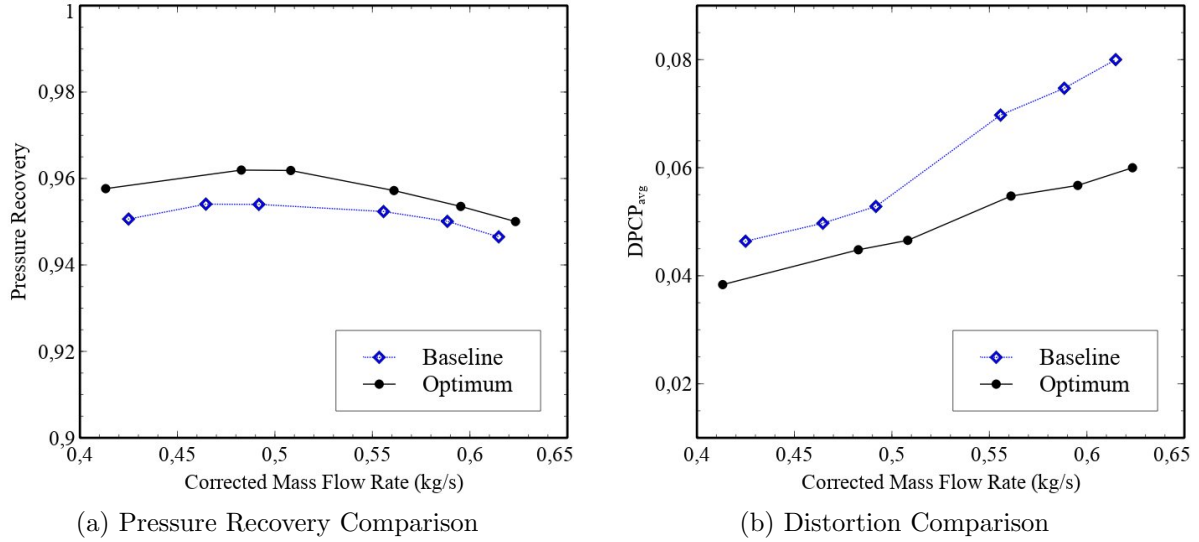
Figure 8: Off-Design Performances

CONCLUSIONS

In this study, adjoint-based optimization is conducted for a semi-submerged inlet exposing a large amount of boundary layer ingestion. Maximizing total pressure recovery at the engine face is taken as the optimization goal. The free-form deformation approach is used for geometrical parametrization with 6699 design variables. Geometrical modifications are only allowed just after the leading edge of the inlet lips. The optimum configuration is able to divert part of the incoming boundary layer away from the inlet entrance. Results indicate that at the design condition 0.82% increase in pressure recovery, 3.32% increase in mass flow rate and 13.21% decrease in distortion is obtained. Investigating the off-design performance of the baseline and the optimum inlets reveals that a similar performance increase is also obtained under off-design conditions.

References

Berrier, B.L., Carter M.L. and Allan, B.G. (2005) *High Reynolds Number Investigation of a Flush-Mounted, S-Duct Inlet With Large Amounts of Boundary Layer Ingestion*, NASA Technical Report, TP-2005-213766, Sep 2005

Kucuk, U.C. and Tuncer, I.H. (2022) *Sınır Tabaka Akışına Maruz Kalan Hava Alığı Geometrisinin Adjoint Yöntem ile Eniyilenmesi*, Ulusal Havacılık ve Uzay Konferansı(UHUK), Sep 2022

Kucuk, U.C.(2022) *Adjoint Based Shape Optimization of Semi-Submerged Inlets and Development of a Novel Boundary Layer Diverter*, PhD dissertation, Middle East Technical University, 2022

Nadarajah, S., and Jameson, A. (2000) *A comparison of the continuous and discrete adjoint approach to automatic aerodynamic optimization*, 38th Aerospace Sciences Meeting and Exhibit. 2000

SAE ARP1420 *Gas Turbine Engine Inlet Flow Distortion Guideline*, Society of Automotive Engineers Report, SAE ARP1420, March 1978

Seddon, J., and Goldsmith, E. L. (1985) *Intake Aerodynamics*, Collins Professional and Technical Books, London, 1985